11-1995

On the Structure and Stability of Geometrical Isomers of N3F

Galina Chaban
Iowa State University

David R. Yarkony
Johns Hopkins University

Mark S. Gordon
Iowa State University, mgordon@iastate.edu

On the Structure and Stability of Geometrical Isomers of N3F

Abstract
The potential energy surfaces for the N_3F molecule have been studied using multiconfigurational wave functions. Two new isomers were found, one on the singlet ($^1A'$) and one on the triplet ($^3A''$) surface. Both isomers have a three-membered cyclic structure and C_s symmetry. The singlet cyclic isomer is endoergic relative to the open fluorine azide by 15–17 kcal/mol. Its kinetic stability is close to the stability of the open isomer: the barrier separating the cyclic isomer from the dissociation products $N_2(X\,^1\Sigma^+_g)$+NF($a\,^1\Delta$) is about 13–17 kcal/mol and is lower than the barrier to isomerization. The triplet cyclic isomer is much higher in energy (about 70 kcal/mol), with a barrier to dissociation to $N_2(X\,^1\Sigma^+_g)$+NF($X\,^3\Sigma^-$) on the order of 15 kcal/mol. Crossings of the $^1A'$ and the $^3A''$ surfaces may allow the cyclic singlet isomer to predissociate to the ground state products, $N_2(X\,^1\Sigma^+_g)$+NF($X\,^3\Sigma^-$). It is shown, however, that the singlet–triplet surface of intersection lies 'behind' the barrier to singlet decomposition, so that spin-forbidden predissociation will not preclude detection of cyclic N_3F.

Keywords
Surface crossings, Dissociation, Dissociation energies, Intermolecular potential energy surfaces, Isomerization

Disciplines
Chemistry

Comments
The following article appeared in *Journal of Chemical Physics* 103 (1995): 7983 and may be found at http://dx.doi.org/10.1063/1.470216.

On the structure and stability of geometrical isomers of N3F

Galina Chaban, David R. Yarkony, and Mark S. Gordon

Citation: The Journal of Chemical Physics **103**, 7983 (1995); doi: 10.1063/1.470216
View online: http://dx.doi.org/10.1063/1.470216
View Table of Contents: http://scitation.aip.org/content/aip/journal/jcp/103/18?ver=pdfcov
Published by the AIP Publishing

On the structure and stability of geometrical isomers of N_3F

Galina Chaban
Department of Chemistry, Iowa State University, Ames, Iowa 50011

David R. Yarkony
Department of Chemistry, Johns Hopkins University, Baltimore, Maryland 21218

Mark S. Gordon
Department of Chemistry, Iowa State University, Ames, Iowa 50011

(Received 11 July 1995; accepted 1 August 1995)

The potential energy surfaces for the N_3F molecule have been studied using multiconfigurational wave functions. Two new isomers were found, one on the singlet ($^1A'$) and one on the triplet ($^3A''$) surface. Both isomers have a three-membered cyclic structure and C_s symmetry. The singlet cyclic isomer is endoergic relative to the open fluorine azide by 15–17 kcal/mol. Its kinetic stability is close to the stability of the open isomer: the barrier separating the cyclic isomer from the dissociation products $N_2(X\ ^1\Sigma_g^+)+NF(a\ ^1\Delta)$ is about 13–17 kcal/mol and is lower than the barrier to isomerization. The triplet cyclic isomer is much higher in energy (about 70 kcal/mol), with a barrier to dissociation to $N_2(X\ ^1\Sigma_g^+)+NF(X\ ^3\Sigma^-)$ on the order of 15 kcal/mol. Crossings of the $^1A'$ and the $^3A''$ surfaces may allow the cyclic singlet isomer to predissociate to the ground state products, $N_2(X\ ^1\Sigma_g^+)+NF(X\ ^3\Sigma^-)$. It is shown, however, that the singlet–triplet surface of intersection lies 'behind' the barrier to singlet decomposition, so that spin-forbidden predissociation will not preclude detection of cyclic N_3F. © *1995 American Institute of Physics.*

I. INTRODUCTION

The very high heat of formation (about 130 kcal/mol) of fluorine azide (NNNF) makes it a candidate as an energetic material. The equilibrium structure of fluorine azide and its decomposition to $N_2(X\ ^1\Sigma_g^+)+NF(a\ ^1\Delta)$ have been studied in a number of experimental and theoretical works.[1–6] It was found that gas phase thermal dissociation of fluorine azide yields metastable $NF(a\ ^1\Delta)$ radicals, and the experimental activation barrier for this dissociation is 15 kcal/mol.[2] Theoretical calculations of the potential energy surface (PES) for the dissociation, including electron correlation via configuration interaction (CI) and fourth-order perturbation theory (MP4) with zero-point energy corrections predict a barrier height of about 12–16 kcal/mol,[4,5] in good agreement with the experimental value. Both experimental and theoretical studies predict a singlet–triplet crossing to lie outside the barrier, that is, in the (product) $N_2(X\ ^1\Sigma_g^+)+NF(X\ ^3\Sigma^-)$ channel.

The low barrier to dissociation (15 kcal/mol) is responsible for the explosiveness of fluorine azide and is the main obstacle to using this compound as an energy source. In this work other regions of the lowest singlet PES of N_3F will be explored in an attempt to identify additional isomers that might be more stable kinetically than fluorine azide. Also considered is the lowest triplet PES and the possibility of radiationless decay attributable to spin–orbit induced coupling of the singlet and triplet states.

Section II contains the theoretical approach. Section III presents the results of our calculations and Sec. IV summarizes and concludes.

II. THEORETICAL APPROACH

The geometrical parameters of the stationary points on the PES's were determined at the restricted Hartree–Fock (RHF), second-order perturbation theory[7] (MP2), single pair generalized valence bond[8] (GVB-1P), and multiconfigurational self-consistent-field[9] (MCSCF) levels of theory using the standard 6-31G(d) basis sets[10] (denoted BASIS-1). Minima and transition states were verified by determining the number of negative eigenvalues (0 for minima; 1 for transition states) of the energy second derivative (Hessian) matrix. The Hessians were determined analytically for RHF, GVB, and MP2 wave functions, and by divided difference of analytic gradients for general MCSCF wave functions. Relative isomer energies were recalculated at higher levels of theory: fourth-order perturbation theory (MP4),[11] quadratic configuration interaction [QCISD(T)],[12] multireference perturbation theory (CASPT2),[13] and multireference configuration interaction (MRCI).[14]

Potential energy surfaces for dissociation (where one can expect considerable configurational mixing) were studied using MCSCF wave functions with (6,6) and (10,10) active spaces. Here the notation (X,Y) denotes all the configuration state functions (CSF's) obtained from distributing X electrons in Y orbitals. The character of these active spaces is discussed in Sec. III. The intrinsic reaction coordinate (IRC) method was used—at the MCSCF(6,6) level with BASIS-1 denoted MCSCF(6,6)/1—to connect all transition states to their corresponding minima. The IRC algorithm used was the second order method developed by Gonzalez and Schlegel[15] with a step size of 0.3 amu$^{1/2}$ bohr. Barrier heights were reevaluated using single point calculations. These calculation were performed using 6-31G(d), 6-311G(d) (denoted BASIS-2) and 6-311G($2d$) (denoted BASIS-3) basis sets[16] at the single reference perturbation theory, MP2 and MP4, and QCISD(T) levels and using MCSCF-based multiconfigurational methods including second-order internally contracted CI [SOICCI—all single and double excitations from

TABLE I. Geometrical parameters. Distances in Å; angles in degrees.

Method	$R(N^1N^2)$	$R(N^2N^3)$	$R(N^3F)$	$\angle N^1N^2N^3$	θ	$N^1N^2N^3F$
			Open isomer 1 ($^1A'$)			
MP2/1	1.154	1.282	1.432	171.6	103.8[a]	180.0
MCSCF(6,6)/1	1.127	1.255	1.377	173.2	104.9[a]	180.0
MCSCF(10,10)/1	1.134	1.278	1.469	175.1	102.1[a]	180.0
			Cyclic isomer 2 ($^1A'$)			
MP2/1	1.249	1.501	1.422	65.4	104.7	
MCSCF(6,6)/1	1.198	1.528	1.358	66.9	105.3	
MCSCF(10,10)/1	1.229	1.500	1.440	65.8	104.7	
MRCI/4	1.213	1.471	1.395	65.7	100.3	
MRCI/5	1.181	1.468	1.383	66.3	101.6	
			Transition state 3 ($^1A'$)[b]			
MCSCF(6,6)/1	1.139	1.904	1.322	72.6	102.5	
MCSCF(10,10)/1	1.149	1.952	1.381	72.9	100.7	
MRCI/4	1.137	1.817	1.383	71.8	100.1	
MRCI/5	1.116	1.760	1.379	71.5	100.4	
			Cyclic isomer 5 ($^3A''$)			
UMP2/1	1.514	1.328	1.388	55.3	133.2	
MCSCF(6,6)/1	1.458	1.368	1.342	57.8	122.9	
			Transition state 6 ($^3A''$)[c]			
MCSCF(6,6)/1	1.416	1.646	1.340	51.1	126.8[a]	−89.5

[a]Angle N^2N^3F.
[b]Transition state for decomposition of 2 ($^1A'$) to N_2+NF($a\ ^1\Delta$).
[c]Transition state for decomposition of 5 ($^3A''$) to N_2+NF($X\ ^3\Sigma^-$).

a (6,6) or (10,10) reference space], MRCI (single and double excitations from reference CSF's), and CASPT2 [second-order perturbation theory with a MCSCF(6,6) or MCSCF(10,10) reference wave function]. Several quantum chemistry programs were used including GAMESS (Ref. 17) for MCSCF calculations, MOLCAS-2 (Ref. 18) for CASPT2, MOLPRO (Ref. 19) for SOICCI and (some) MRCI, and GAUSSIAN-92 (Ref. 20) for MP2, MP4, and QCISD(T) calculations.

For reasons described later, a section of the surface of intersection for the lowest singlet and triplet states was explored using methods developed by Yarkony and co-workers.[21] The states were described at the MRCI level. The nitrogen $1s$ and fluorine $1s$ and $2s$ orbitals were kept doubly occupied. The remaining 20 electrons were distributed among the [active1(5–11 a',2–3 a''), active2(12 a', 4–5 a''), virtual] orbitals as [18,2,0] [17,3,0], [16,4,0], [18,1,1], [17,2,1], [18,0,2], [17,1,2], and [16,2,2]. The four molecular orbitals with the highest orbital energies were excluded from the virtual space. All CSF's arising from these electron configurations were included in the MRCI expansion. The molecular orbitals were in turn determined from CAS state-averaged MCSCF calculations using the active2 space. The character of the active orbitals is discussed in Sec. III (see Table III and Fig. 3). These calculations were performed using [$4s2p1d$] Dunning double zeta polarization,[22] and [$5s4p1d$] McLean and Chandler bases,[23] denoted BASIS-4 and BASIS-5 respectively. These levels of treatment will be denoted MRCI/4 and MRCI/5, respectively. Here and throughout this work the designation M/J will refer to a calculation performed at level of theory (or method) M using BASIS-J. Additional calculations were performed at the CCSD(T) level of theory (Ref. 24), with two basis sets, 6-311++G(d,p) (Ref. 20) (BASIS-6) and 6-311+ +G($2df,2pd$) (Ref. 16) (BASIS-7) and at the MRCI level using $5s4p2d$ (Ref. 25) bases (BASIS-8).

III. RESULTS

A. Structural isomers

The key result of this work is the discovery of a new metastable cyclic isomer of N_3F that is endoergic relative to the open isomer N–N–N–F [see Table I and Fig. 1, structure 1 ($^1A'$)]. This new isomer has a three-membered cyclic structure with C_s symmetry [see Fig. 1, structure 2 ($^1A'$)]. Geometrical parameters for this cyclic isomer are shown in Table I. The MP2/1 and MCSCF(10,10)/1 levels of theory predict

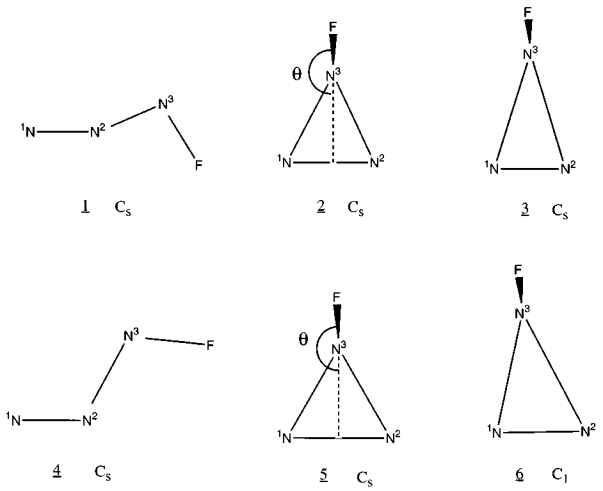

FIG. 1. Structures of the stationary points on the PES's of singlet and triplet N_3F. Singlet: 1,2-minima, 3-transition state; triplet: 4,5-minima, 6-transition state.

TABLE II. Energetics. Total energies in hartrees; relative energies in kcal/mol.

	2 ($^1A'$)		1 ($^1A'$)	3 ($^1A'$)	N_2+NF($a\ ^1\Delta$)
Method	E^{tot}	E^{rel}	E^{rel}	E^{rel}	E^{rel}
MCSCF(6,6)/1[a]	−262.698 93	0.0	−1.1	10.6	−24.5
SOICCI(6,6)/1[b]	−262.755 20	0.0		11.2	−14.5
MRCI(6,6)/1[b]	−263.197 29	0.0		12.2	−12.0
CASPT2(6,6)/1[b]	−263.244 80	0.0	−16.7	13.2	−12.4
MCSCF(10,8)/1[b]	−262.709 92	0.0		6.9	−19.7
CASPT2(10,8)/1[b]	−263.247 70	0.0		12.8	−11.6
MCSCF(10,10)/1[c]	−262.791 17	0.0	−2.0	18.0	−11.9
SOICCI(10,10)/1[c]	−262.904 89	0.0		20.1	0.1
CASPT2(10,10)/1[c]	−263.249 97	0.0	−15.4	16.9	−8.4
MCSCF(14,12)/1[c]	−262.807 26	0.0		10.7	−18.7
MCSCF(10,10)/2[c]	−262.859 04	0.0		18.3	−14.1
CASPT2(10,10)/2[c]	−263.453 32	0.0		17.6	−11.0
MCSCF(10,10)/3[c]	−262.869 48	0.0		16.7	−14.2
CASPT2(10,10)/3[c]	−263.507 53	0.0		13.7	−13.7
MP2/1	−263.243 93	0.0	−16.5		
MP4/1[d]	−263.282 86	0.0	−16.4		
QCISD(T)/1[d]	−263.276 68	0.0	−15.1		
MRCI/4[a]	−263 117 462	0.0		19.1	
MRCI/5[a]	−263.156 100	0.0		11.3	
	5 ($^3A''$)			6 ($^3A''$)	N_2+NF($X\ ^3\Sigma^-$)
MCSCF(6,6)/1[a]	−262.560 99	86.6		96.2	−65.7
CASPT2(6,6)/1[b]	−263.151 51	57.3		74.4	−49.9
MCSCF(10,10)/1[b]	−262.659 29	82.8		95.8	−54.8
CASPT2(10,10)/1[b]	−263.152 76	61.0		77.3	−45.2
MP2/1[a]	−263.140 24	65.1			
MP4/1[d]	−263.172 09	69.5			
QCISD/1[d]	−263.174 76	63.9			

[a]Structure optimized at indicated level.
[b]Based on the MCSCF(6,6)/1 geometry.
[c]Based on the MCSCF(10,10)/1 geometry.
[d]Based on the MP2/1 geometry.

very similar geometries, while the MRCI/4 and MRCI/5 bond distances are only slightly shorter. The cyclic isomer 2 ($^1A'$) has one N═N double bond, $R(N^1N^2)\sim1.2$ Å compared to $r_e[N_2(X\ ^1\Sigma_g^+)]=1.10$ Å,[26] and two weak N–NF single bonds. The NF group, $R(N^3F)\sim1.35$ Å compared to $r_e[NF(a^1\Delta)]=1.31$ Å,[26] forms an angle ($\equiv\theta$) of ~105° with the plane of the ring. This structure was verified to be a minimum at all levels of theory used in this paper.

Two structures [open 4 ($^3A''$) and cyclic 5 ($^3A''$)] were also found to be local minima on the triplet PES at the ROHF/1 and UHF/1 levels (see Fig. 1). However, at the Hartree–Fock level of theory the open structure is very weakly bound and separated from dissociation products by a barrier of only 3–4 kcal/mol. At the MP2 level this structure is not stable. Therefore, this open structure was not pursued at higher levels of theory. Figure 1 and Tables I and II give the geometrical parameters and energies of the cyclic triplet structure 5 ($^3A''$). The triplet cyclic isomer is very high in energy, about 70–80 kcal/mol higher than the ground state singlet open isomer at MP2/1 and CASPT2/MCSCF(6,6)/1 levels of theory. Although it is stable kinetically (see the following), it will decay radiatively to the ground singlet state.

B. Decomposition of cyclic isomers

The decomposition of cyclic N_3F to $N_2(X\ ^1\Sigma_g^+)+NF(a\ ^1\Delta)$ was studied using multiconfigurational wave functions with active spaces ranging from (6,6) to (14,12). The minimum active space (6,6) necessary for a correct qualitative description of the dissociation process includes three bonding orbitals (the $10a'$, $11a'$, and $4a''$ orbitals, corresponding to two N_2–NF bonds and the N–N π bond) and the three corresponding antibonding orbitals (the $5a''$, $6a''$, and $12a'$ orbitals). Upon dissociation these orbitals convert to two π (N–N), two π^*(N–N), and two π^*(N–F) orbitals. The MCSCF(6,6)/1 treatment was used to locate the transition state and analyze the IRC path connecting the transition state with the cyclic isomer and products of dissociation. The energy along the IRC path is shown in Fig. 2. From Fig. 2 it is seen that the IRC is dominated by $R(N_2$–NF). The MCSCF natural orbitals are shown in Fig. 3, and the corresponding occupation numbers are listed in Table III. It is seen from Table III that the occupation number of the $4a''$ orbital decreases from 1.93 (essentially doubly occupied) in the cyclic isomer to 1.0 in the dissociation products. Simultaneously, the $12a'$ orbital increases its occupation from 0.05 to 1.0. Thus, this wave function dissociates to $N_2(X\ ^1\Sigma_g^+)+NF(a\ ^1\Delta)$ with two half occupied π^*(N–F) orbitals.

With the foregoing information in hand the energetics were reinvestigated using larger basis sets and more flexible wave functions. These results are collected in Table II. The geometry of the transition state was reoptimized at the MCSCF(10,10) level. The bigger active space was constructed

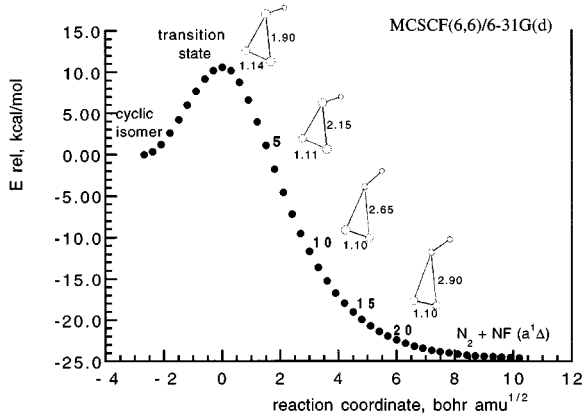

FIG. 2. MCSCF(6,6)/6-31G(d) reaction path for decomposition of singlet cyclic N_3F.

by adding two bonding orbitals: $\sigma(N^1–N^2)$ and $\sigma(N^3–F)$, and the two corresponding antibonding orbitals to the (6,6) active space. The transition state at the MCSCF(10,10) level is similar to the MCSCF(6,6) level result, although $R(N^3–F)$ and $R(N^2–N^3)$ increase by 0.06 and 0.05 Å respectively, see Table I.

The height of the barrier to dissociation was recalculated using the CASPT2 method with (6,6), (10,10), and(10,8) active spaces using BASIS-1. Unlike the (10,10) active space the (10,8) active space added two doubly occupied nitrogen lone pairs to the (6,6) active space. Upon dissociation, these lone pairs become two π(N–F) orbitals. Single point CASPT2 (10,10) calculations were also performed using BASIS-2 [6-311G(d)] and BASIS-3 [6-311G(2d)]. As seen in Table II, there is little variation in the CASPT2 predicted barrier heights, as a function of active space or basis set. The predicted barrier is in the 13–17 kcal/mol range. The barrier height is discussed further below. The exothermicity of the dissociation from the cyclic isomer is predicted to be 11–14 kcal/mol at the CASPT2/2 and CASPT2/3 levels.

TABLE III. MCSCF natural orbital occupation numbers. The orbitals are shown in Fig. 3.

Orbital	$10a'$	$11a'$	$4a''$	$5a''$	$6a''$	$12a'$
Cyclic	1.914	1.943	1.929	0.086	0.078	0.050
Transition state	1.927	1.897	1.900	0.073	0.104	0.099
Point 5	1.934	1.929	1.678	0.066	0.071	0.322
Point 10	1.935	1.934	1.314	0.065	0.066	0.686
Point 15	1.935	1.934	1.101	0.065	0.066	0.899
Point 20	1.935	1.935	1.020	0.065	0.065	0.980
Point 27	1.935	1.935	0.992	0.065	0.065	1.008

The dissociation of the triplet cyclic isomer to $N_2(X\ ^1\Sigma_g^+)$ and $NF(X\ ^3\Sigma^-)$ was studied at the MCSCF(6,6)/1 level. The transition state located at this level of theory has no symmetry. Its structure $\underline{6}$ ($^3A''$) is shown in Fig. 1, and the geometrical parameters are given in Table I. Note that the $R(N^iN^3)$, $i=1,2$ are considerably shorter in the cyclic triplet than in the corresponding singlet. The reaction path for the dissociation is shown in Fig. 4. The height of the barrier estimated by a single point CASPT2/MCSCF(10,10)/1 calculation at the MCSCF(6,6)/1 geometry is ~16 kcal/mol, and the exothermicity of the reaction is about 106 kcal/mol.

The triplet cyclic isomer $\underline{5}$ ($^3A''$) is 61 kcal/mol higher in energy than the corresponding singlet $\underline{2}$ ($^1A'$) at the CASPT2(10,10)/1 level. At the same level of theory, the asymptote $N_2(X\ ^1\Sigma_g^+)+NF(X\ ^3\Sigma^-)$ is 36.8(36.95) kcal/mol *below* the singlet asymptote, $N_2(X\ ^1\Sigma_g^+)+NF(a\ ^1\Delta)$, in excellent agreement with the experimental value[26] given parenthetically. Thus the $1\ ^1A'$ and $1\ ^3A''$ potential energy surfaces must cross. This crossing may lead to spin-forbidden predissociation of the $\underline{2}(^1A')$ moiety. Note that the energy recovered from singlet cyclic N_3F would be 45, rather than 8, kcal/mol if the spin-forbidden path were followed. At the singlet transition state $E(1\ ^1A')-E(1\ ^3A'')\sim-1$ kcal/mol at the CASPT2(10,10)/1 level of theory, suggesting a crossing in this region. However larger singlet–triplet separations, ~37 kcal/mol, are observed using coupled cluster wave functions (see the following discussion). Thus a more precise

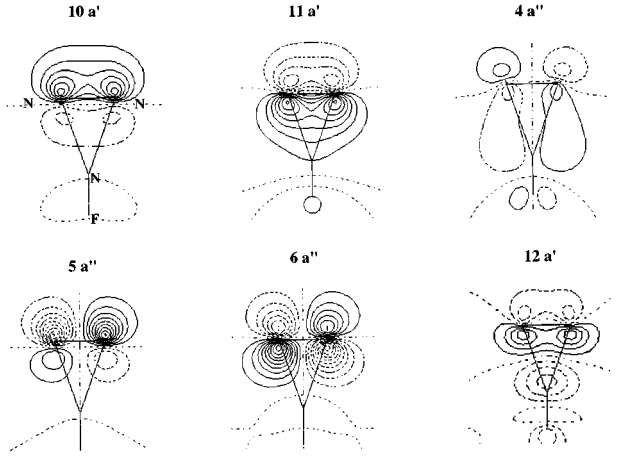

FIG. 3. MCSCF/6-31G(d) natural orbitals for singlet transition state $\underline{3}$ in the plane of the N_3 ring.

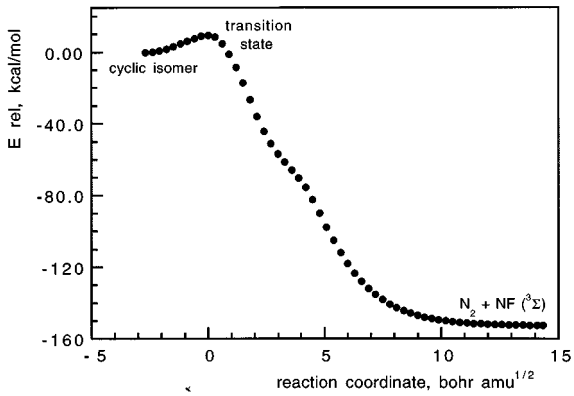

FIG. 4. MCSCF(6,6)/6-31G(d) reaction path for decomposition of triplet cyclic N_3F.

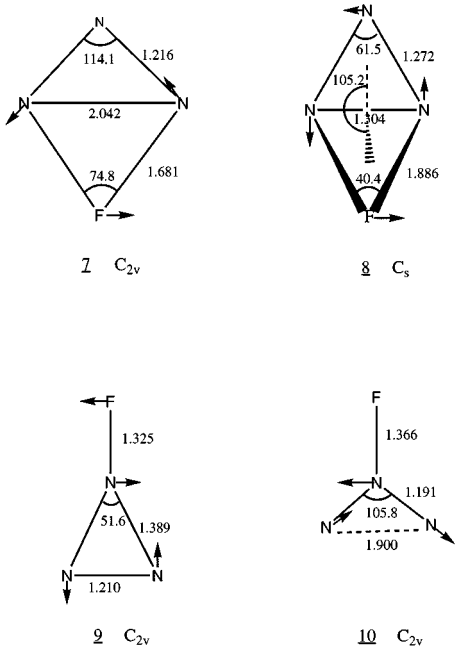

FIG. 5. RHF/6-31G(d) geometries for transition states of rearrangements on the singlet PES of N_3F.

description of the surface of intersection is desirable. This point is addressed in Sec. III D.

C. Rearrangements between isomers on the singlet potential energy surface

Attempts to locate a transition state for the rearrangement between the open and cyclic isomers on the singlet PES were unsuccessful at all calculational levels except for GVB(1P)/1. The height of the isomerization barrier at the GVB(1P)/1 level was found to be 11.5 kcal/mol (from the cyclic isomer). This is close to the barrier height for dissociation of the cyclic isomer at this computational level (11.8 kcal/mol). At the MCSCF(6,6)/1 and MP2/1 levels of theory, the cyclic isomer dissociates to $N_2(X\ ^1\Sigma_g^+)+NF(a\ ^1\Delta)$ before it reaches the isomerization transition state. It is likely that the barrier for isomerization from the cyclic isomer is higher than the barrier to dissociation of this isomer, and therefore that the intramolecular rearrangement between the cyclic and open singlet isomers does not occur.

Four other transition states have been found on the singlet potential energy surface at the RHF/1 and GVB(1P)/1 levels. Partial geometries and imaginary modes for these structures are shown in Fig. 5. Following the GVB(1P) IRC from transition state 7 ($^1A'$) illustrates that this species corresponds to the degenerate rearrangement between two open isomers. Similarly, transition state 8 ($^1A'$), the nonplanar bicyclic structure, corresponds to a degenerate rearrangement between two cyclic isomers, with the F atom moving from one N atom to another. The GVB(1P) barriers for these rearrangements are quite high: 58 and 78 kcal/mol, respectively. The C_{2v} structures 9 ($^1A'$) and 10 ($^1A'$) (142 and 100 kcal/mol higher, respectively, than the open isomer) are found to be transition states between two open isomers at the GVB(1P) level of theory. Since all four structures 7–10 are much higher in energy than the transition states for dissociation of both the open and cyclic isomers, such rearrangements are extremely unlikely and were not pursued at higher levels of theory.

TABLE IV. MRCI/5 analysis of singlet–triplet surface of intersection. E_x in kcal/mol relative to $E(^1A')=-263.156\,100$ a.u. at MRCI/5 2 ($^1A'$) structure. $\Delta E=|E(1\ ^1A')-E(^3A'')|<1\ cm^{-1}$.

	$R(N^1N^2)$	$R(N^2N^3)$	$R(N^3F)$	$\angle N^1N^2N^3$	θ	E_x
MECP	1.089	1.869	1.371	73.0	99.3	5.3
$X(N–N^1)$	1.058	1.826	1.381	73.2	117.7	17.5
$X(N–N^1)$	1.060	1.757	1.416	72.4	134.2	37.3

D. Singlet–triplet surface of intersection

The vibrational levels of cyclic $N_3F(^1A')$ are, technically speaking, resonances since they can be predissociated to $N_2(X\ ^1\Sigma_g^+)+NF(X\ ^3\Sigma^-)$ through spin–orbit interactions with the $^3A''$ state. The lifetime of the vibrational levels is determined by the relation between the $^1A'-{}^3A''$ surface of intersection and the coordinate space on the $^1A'$ surface sampled by the vibrational wave function. It is important to distinguish two situations, one in which the state lives long enough (for example, microseconds) to be detected and the second in which the state lives long enough (for example, days) to be useful as an energetic species, with the latter situation requiring a more detailed analysis than the former.

From Table I it is seen that the principal difference between the equilibrium structure of cyclic N_3F and its transition state for decomposition to $N_2(X\ ^1\Sigma_g^+)+NF(a\ ^1\Delta)$ is attributable to changes in $R(N^1N^3)$ $[=R(N^2N^3)]$. For this reason the $^1A'-{}^3A''$ surface of intersection was characterized as a function of $R(N^1N^3)$, which represents an approximate reaction coordinate—see Fig. 2. Three points on the surface of intersection, at the MRCI/5 level, are reported in Table IV: (i) The minimum energy crossing point (MECP), a local minimum on the $^1A'-{}^3A''$ surface of intersection, for which $R(N^1N^3)=1.869$ Å, and two additional points with $R(N^1N^3)$ fixed at (ii) its MRCI/5 transition state value, $R(N^1N^3)=1.757$ Å, and (iii) an intermediate value, $R(N^1N^3)=1.826$ Å. In each case the remaining geometric parameters were optimized to minimize the common energy $E(^3A'')(\mathbf{R})=E(^1A')(\mathbf{R})\equiv E_x(\mathbf{R})$. It is seen by comparing Tables II and IV that the MECP is lower in energy than the transition state and, significantly, differs from the transition state structure principally in the value of $R(N^1N^3)$. However, since $R(N^1N^3)$ is larger at the MECP than at the transition state, the MECP lies "behind" the barrier to spin-allowed dissociation. Furthermore as $R(N^1N^3)$ decreases toward its value at the transition state, the energy of the intersection point increases rapidly, so that in a qualitative sense the crossing surface is either "behind," or well above, the barrier to spin-allowed dissociation. Since the $^1A'-{}^3A''$ surface of intersection can only be reached by tunneling through the barrier on the $^1A'$ surface or at significant energetic cost, spin-forbidden predissociation will not prevent observation

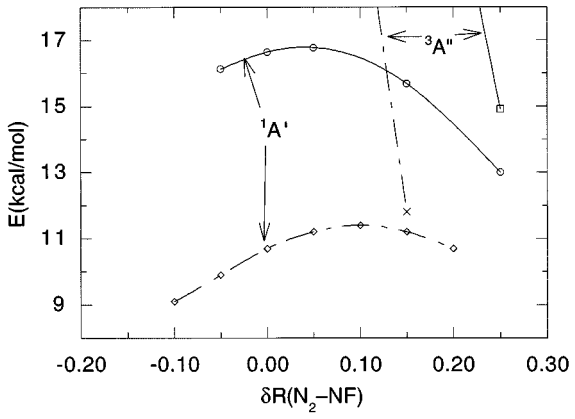

FIG. 6. $E(^1A')$ and $E(^3A'')$ as function of $\delta R(N_2\text{–}NF) \equiv R(N_2\text{–}NF) - R(N_2\text{–}NF)(TS)$. $R(N_2\text{–}NF)(TS)$ obtained at MRCI/5 level. Solid curves at MRCI/8 level; dashed curves at CCSD(T)/6 level.

of cyclic N_3F. The lifetime of the individual vibrational levels with respect to spin-forbidden predissociation will be the object of a future publication.

The behavior of the $^1A'$ and $^3A''$ potential energy surfaces in the vicinity of the transition state and MECP (MRCI/5 level) is illustrated from an alternative perspective in Fig. 6 which reports $E(^1A')$ and $E(^3A'')$ as a function of $R(N_2\text{–}NF)$ at the MRCI/8 level, with the remaining coordinates fixed at their transition state (MRCI/5 level) values. From Fig. 6 it is seen that $\Delta E(^3A'',^1A') \equiv E(^3A'') - E(^1A')$ depends very sensitively on $R(N_2\text{–}NF)$. Thus the precise energy of a crossing point is expected to depend on the level of theory used to characterize the $^1A'$ and $^3A''$ states. To address this question the $^1A'$ and $^3A''$ states were studied in this region using CCSD(T) wave functions. Calculations performed with BASIS-6[6-311++G(d,p)] and BASIS-7[6-311++G$(2df,2pd)$] are reported Table V and Fig. 6. Since the triplet state energies were calculated using unrestricted Hartree–Fock (UHF) wave functions as the starting point, it is important to note that the spin contamination for all calculations is small, with $\langle S^2 \rangle \leqslant 2.04$. At the transition state the $^1A'$ and $^3A''$ state are separated by ~39 kcal/mol. However, at the MECP geometry the separation is reduced to 5.7 kcal/mol (BASIS-6) and 8.5 kcal/mol (BASIS-7). Still these are fairly large splittings. To understand their origin $R(N_2\text{–}NF)$ was varied from its MRCI/5 value ($[R(N_2\text{–}NF)]=1.87$ Å) in steps of 0.01 Å, using BASIS-6. In these calculations remaining geometrical parameters were fixed. When $R(N_2\text{–}NF)$ is increased by only 0.03 Å, to 1.90 Å, the singlet-triplet splitting decreases to 0.1 kcal/mol! Note that both the MRCI/8 and CCSD(T)/6 data reported in Fig. 6 suggest that the MRCI/5 treatment underestimates the energy at the MECP.

TABLE V. CCSD(T) Analysis of vicinity of singlet–triplet surface of intersection. Eq., equilibrium structure; TS and MECP from the MRCI/5 treatment. Relative energies in kcal/mol. $E(\text{Eq.}) = -263.404\,58$ a.u. for CCSD(T)/6 treatment, and $-263.539\,28$ a.u. for CCSD(T)/7 treatment. TS(MECP)+x=TS(MECP) structure with $R(N_2\text{–}NF)$ increased by x Å as discussed in text.

	$^1A'$		$^3A''$	
Structure	CCSD(T)/6	CCSD(T)/7	CCSD(T)/6	CCSD(T)/7
Eq.	0.0	0.0	103.7	102.9
TS	10.7	9.9	47.0	48.8
TS+0.05	11.2		33.7	
TS+0.10	11.4		22.0	
TS+0.15	11.2		11.8	
MECP	15.0	14.1	20.7	22.6
MECP+0.01	14.9		18.4	
MECP+0.02	14.7		16.4	
MECP+0.03	14.6		14.4	

The CCSD(T)/6 calculations in the vicinity of the MECP also indicate (as do the MRCI/5 results from Table I and the MRCI/8 results in Fig. 6) that at the transition state $R(N^1N^3)$ is somewhat shorter than the ~1.9–1.95 Å suggested by MCSCF(6,6) and MCSCF(10,10). Since analytic CCSD(T) gradients are not available to us, this last point was explored by analyzing the CCSD(T)/6 potential energy surface in the vicinity of the MRCI/5 transition state. To this end, $R(N_2\text{–}NF)$ was varied in steps of ± 0.05–± 0.20 Å, from the MRCI/5 transition state, with all other geometric parameters held fixed. Exploratory changes in $R(N^3F)$ suggest that this is a reasonable procedure. The results are presented in Table V and Fig. 6. It was found by this procedure that the CCSD(T) transition state should have $R(N_2\text{–}NF) \approx 1.86$ Å. The locus of the transition state and crossing point at the CCSD(T)/6 level are consistent with the previous assertion that the relevant portion of $^1A' - {}^3A''$ surface of intersection occurs behind (or above) the barrier to spin-allowed dissociation, see Fig. 6. Thus the key conclusion of this subsection, that the surface of intersection is ''behind'' or above the barrier to spin-allowed dissociation, is supported at all levels of treatment.

The previous discussion has focused on the single coordinate $R(N_2\text{–}NF)$. It is interesting to ask how effective are the remaining degrees of freedom in changing $\Delta E(^3A'',^1A')$. Analysis of the energy difference gradient, $(\partial/\partial R_\alpha)[\Delta E(^3A'',^1A')]$, shows that in the immediate vicinity of the MECP the singlet–triplet separation is most sensitive to $R(N_2\text{–}NF)$ and secondarily to $R(N^1N^2)$ (equivalently, it is sensitive to both the coordinates $R(N^1N^3)$ and $\angle N^1N^2N^3$). It is much less sensitive to θ and $R(N^3F)$. However as $R(N^1N^3)$ decreases, the N_2–NF interaction increases so that θ and $R(N^3F)$ play a more significant role in characterizing the surface of intersection. These observations are reflected in the data in Table IV.

Table V reports two points near the $^1A' - {}^3A''$ surface of intersection at the CCSD(T)/6 level, denoted TS+0.15 and MECP+0.03, with similar energies ~11.5 and ~14.5 kcal/mol, respectively. The small energetic difference reflects that fact that $R(N_2\text{–}NF)$ is virtually identical for these two points, being 1.819 and 1.817 Å respectively. Thus these results are consistent with the geometry dependence of $E_x(\mathbf{R})$ in Table IV and the discussion in the preceding paragraph.

IV. SUMMARY AND CONCLUSIONS

The potential energy surfaces for the N_3F molecule have been studied using multiconfigurational wave functions. Two new isomers were found: one on the singlet and one on the triplet, PES. Both isomers have a three-membered cyclic

structure and C_s symmetry. The singlet cyclic isomer is endoergic relative to the open fluorine azide by 15–17 kcal/mol. Its kinetic stability is close to the stability of the open isomer: the barrier separating the cyclic isomer from the dissociation products $N_2(X\ ^1\Sigma_g^+)+NF(a\ ^1\Delta)$ is between 11–17 kcal/mol and is lower than the barrier to isomerization. The triplet cyclic isomer is much higher in energy (about 70 kcal/mol), with a barrier to dissociation to $N_2(X\ ^1\Sigma_g^+)+NF(X\ ^3\Sigma^-)$ on the order of 15 kcal/mol.

The triplet dissociation products, $N_2(X\ ^1\Sigma_g^+)+NF(X\ ^3\Sigma^-)$, are ~37 kcal/mol lower in energy than the singlet products, $N_2(X\ ^1\Sigma_g^+)+NF(a^1\Delta)$, consequently crossing of the $^1A'$ and the $^3A''$ surfaces may allow the cyclic singlet isomer to predissociate to the ground state products, $N_2(X\ ^1\Sigma_g^+)+NF(X\ ^3\Sigma^-)$. It was found that the singlet-triplet surface of intersection lies "behind" the barrier to singlet decomposition. Thus spin-forbidden predissociation will not preclude detection of cyclic N_3F. Additional studies are required to determine whether spin forbidden radiationless decay will affect the utility of cyclic N_3F as an energetic fuel.

ACKNOWLEDGMENTS

This work was supported by grants from the Air Force Office of Scientific Research, Grant No. F49620-95-1-0077, to M.S.G. and, Grant No. F49620-93-1-0067, to D.R.Y. Calculations were performed on IBM RS 6000/350 and 370 workstations, generously provided by Iowa State University and on IBM RS 6000/580 and 590 workstations at Johns Hopkins University. Many helpful discussions with Dr. Kiet Nguyen are gratefully acknowledged.

[1] N. J. S. Peters, L. C. Allen, and R. A. Firestone, Inorg. Chem. **27**, 755 (1988).
[2] D. Christen, H. G. Mack, G. Schatte, and H. Willner, J. Am. Chem. Soc. **110**, 707 (1988).
[3] D. J. Benard, B. K. Winker, T. A. Seder, and R. H. Cohn, J. Phys. Chem. **93**, 4790 (1989).
[4] H. H. Michels and J. A. Montgomery, *Proceedings of the High Energy Density Materials Contractors Conference* (AFOSR, Washington, D.C., 1989).
[5] N. R. Kestner, N. E. Brener, and J. Callaway, *Proceedings of the High Energy Density Materials Contractors Conference* (AFOSR, Washington, D.C., 1990).
[6] M. Otto, S. D. Lotz, and G. Frenking, Inorg. Chem. **31**, 3647 (1992).
[7] J. A. Pople, J. S. Binkley, and R. Seeger, Int. J. Quantum Chem. **10**, 1 (1976).
[8] W. A. Goddard, T. H. Dunning, W. J. Hunt, and P. J. Hay, Acc. Chem. Res. **6**, 368 (1973).
[9] B. Lam, M. W. Schmidt, and K. J. Ruedenberg, Phys. Chem. **89**, 2221 (1985).
[10] W. J. Hehre, R. Ditchfield, and J. A. Pople, J. Chem. Phys. **56**, 2257 (1972).
[11] R. Krishnan, M. J. Frisch, and J. A. Pople, J. Chem. Phys. **72**, 4244 (1980).
[12] J. A. Pople, M. Head-Gordon, and K. J. Raghavachari, Phys. Chem. **87**, 5968 (1987).
[13] K. Anderson, P.-A. Malmqvist, and B. O. Roos, J. Chem. Phys. **96**, 1218 (1992); K. Anderson, P.-Å, Malmqvist, and B. O. Roos, J. Phys. Chem. **94**, 5483 (1990).
[14] H.-J. Werner and P. J. Knowles, J. Phys. Chem. **89**, 1988 (1988); P. J. Knowles and H.-J. Werner, Chem. Phys. Lett. **145**, 514 (1988).
[15] C. Gonzalez and H. B. Schlegel, J. Chem. Phys. **90**, 2154 (1989); J. Phys. Chem. **94**, 5523 (1990); J. Chem. Phys. **95**, 5853 (1991).
[16] P. C. Hariharan and J. A. Pople, Theor. Chim. Acta. **28**, 213 (1973); R. Krishnan, J. S. Binkley, R. Seeger, and J. A. Pople, J. Chem. Phys. **1980**, 72, 650 (1980); M. J. Frisch, J. A. Pople, and J. S. Binkley, *ibid*. **80**, 3265 (1984).
[17] M. W. Schmidt, K. K. Baldridge, J. A. Boatz, S. T. Elbert, M. S. Gordon, J. H. Jensen, S. Koseki, N. Matsunaga, K. A. Nguyen, S. Su, and T. L. Windus, J. Comp. Chem. **14**, 1347 (1993).
[18] K. Anderson, M. P. Fülscher, R. Lindh, P.-Å. Malmqvist, J. Olsen, B. O. Roos, A. J. Sadlej, and P.-O. Wilmark, MOLCAS version 2, User's Guide; University of Lund, Sweden, 1991.
[19] MOLPRO is written by H.-J. Werner and P. J. Knowles, with contributions by J. Almlöf, R. D. Amos, S. T. Elbert, and P. R. Taylor.
[20] GAUSSIAN 92, Revision C, M. J. Frisch, G. W. Trucks, M. Head-Gordon, P. M. W. Gill, M. W. Wong, J. B. Foresman, B. G. Johnson, H. B. Schlegel, M. A. Robb, E. S. Replogle, R. Gomperts, J. L. Andres, K. Raghavachari, J. S. Binkley, C. Gonzalez, R. L. Martin, D. J. Fox, D. J. Defrees, J. Baker, J. J. P. Stewart, and J. A. Pople, Gaussian, Inc., Pittsburgh, PA, 1992.
[21] D. R. J. Yarkony, Am. Chem. Soc. **114**, 5406 (1992); D. R. J. Yarkony, Chem. Phys. **92**, 2457 (1990); D. R. Yarkony, Int. Rev. Phys. Chem. **11**, 195 (1992).
[22] T. H. Dunning, and P. J. Hay, in *Gaussian Basis Sets for Molecular Calculations*, in *Modern Theoretical Chemistry*, edited by H. F. Schaefer (Plenum, New York, 1976).
[23] A. D. McLean and G. Chandler, J. Chem. Phys. **72**, 5639 (1980); (private communication). The $[5s4p1d]$ bases used in this study can be found in D. R. Yarkony, J. Chem. Phys. **85**, 7261 (1986).
[24] See, for example, R. J. Bartlett, J. Phys. Chem. **93**, 1697 (1989), and references cited therein.
[25] $5s4p2d$ bases are the $5s4p$ bases of McLean and Chandler with two sets of d functions from R. Ahlrichs, P. Scharf, and K. Jankowski, Chem. Phys. **98**, 381 (1985).
[26] K. P. Huber and G. Herzberg, *Molecular Spectra and Molecular Structure IV. Constants of Diatomic Molecules* (Van Nostrand Reinhold, New York, 1979).